Transport and carrier injection effects of junction in spin-orbit coupling heterojunction using resonance force microscopy

R. REN*, WEIREN WANG, XUAN LI, ZHONGXIA ZHAO
Department of optics, Xi'an Jiao Tong University, Xian, 710054, China

Carrier transport effect was displayed between ZnO and $LaGdSrCoO_3$ thin films epitaxially grown on $LaAlO_3$ (100) substrates by pulse laser deposit. The photo-responsive resistance irradiated by 300fs laser pulse and magnetoresistance in fabricated $ZnO/LGSrCO_{3+\sigma}/LaAlO_3$ heterostructure were presented at 80-300 K. The ZnO/LGSCO heterojunction exhibited the carrier transfer of MIT transition and photoinduced demagnetization. The ZnO/LGSCO junction showed rectifying behavior at 80-300 K. Additionally, the heterostructure showed a positive colossal magnetoresistance (MR) effect over the range of 50–300 K which MR increased 5.32% at 0.5T and 4.62% at 0.2T, 100 K and a PR effect over the range of. 50–210 K.

(Received May 1, 2013; accepted July 11, 2013)

Keywords: Carrier injection, Spin-orbit, Photoinduced demagnetization, MIT transition

1. Introduction

$R_{1-x}A_xCoO_3$ colossal magnetoresistance oxides that show ferroelectric and antiferromagnetic ordering with the formula of perovskite type simultaneously are currently attracting intensive investigations due to their interesting fundamental physics as well as potential applications in information storage and spintronics. For magnetoresistance heterostructures, R rare earth elements are partially doped in proportion to the A divalent alkaline earth compound. The doped manganese oxides $ZnO/La_{0.4}Gd_{0.1}Sr_{0.5}CoO_{3+\sigma}$ junction of carrier transfer were modified by electron spin order, orbital order, and lattice field to exhibit photoinduced resistance and colossal magnetoresistance (CMR) effect [1-2,4-7]. Lu reported positive magnetoresistance and high MR sensitivity of $La_{0.9}Sr_{0.1}MnO_3$ /$SrNb_{0.01}Ti_{0.99}O_3$ in modulated low magnetic fields [25]. Pabst focused on mechanisms, which led to the large leakage current in high quality BFO thin films to integrate BFO into functional microelectronic devices [15]. Arindam used nonequilibrium magnetotransport spectroscopy to explore spin polarization at low temperature and a strong sensitivity of such polarization to magnetic fields [13]. Wu reported that the resistive hysteresis and the rectification ratio of diodelike behavior in bilayered BFO/ZnO thin films were enhanced with increasing electrical field and temperature [14]. For $ZnO/La_{0.4}Gd_{0.1}Sr_{0.5}CoO_{3+\sigma}$ films, the antiferromagnetic insulator LaCoO doped Gd and Sr displayed difference proportion of Co^{3+} and Co^{4+}. The control of doped Gd concentration through the junction $ZnO/La_{0.4}Gd_{0.1}Sr_{0.5}CoO_3$ could alter interfacial energy band, and achieved antiferromagnetic insulator transition from ferromagnetic metal [5,6]. The $La_{1-x}Sr_xCoO_3$ films could display changed-ordering properties among ferromagnetic state, paramagnetism and spin glass depending on the thermal and magnetic history and grain boundary resistance, oxygen air ambient and crystallographic structure [7,12]. However, x=0.5 and double doped Gd, Sr $LaABCoO_3$ and ZnO/LGSCO junction are few being reported. The phase transition and spin-orbit coupling mechanism of ZnO/LGSCO heterojuction are little explored from the direction of junction CMR effect in the past few years.

In this work, we reported the fabrication of p-n heterojunction of cobalt perovskites $La_{0.4}Gd_{0.1}Sr_{0.5}CoO_{3+\sigma}$ and ZnO fabricated by pulse laser deposition consisted of n-type ZnO and p-type $La_{0.4}Gd_{0.1}Sr_{0.5}CoO_{3+\sigma}$ grown on LaAlO substrate. In order to investigate junction ferromagnetic phase transition and insult to metal, we prepared multi-crystal LGSCO/ZnO to introduce MR and photocarrier injection. A temperature dependence of photoresistance and positive magnetoresistance was observed in this junction that has some special properties of ferromagnetic semiconductor [8, 9], multilevel resistive switching [10], positive colossal magnetoresistance [11, 12], colossal electroresistance [13], manganite tunnel junctions [14], high magnetic sensitivity [15] and ultraviolet fast-response [16]. The junction showed photocarrier injection properties, and the light dynamic controls electrons carrier transport from ZnO to LGSCO in which hole concentration decreased owing to electron injection following the photoexcitation of ZnO and Si.

2. Experiments

For the study, the ZnO was sintering at 500°C for 48h by solid state reaction. The target $La_{0.4}Gd_{0.1}Sr_{0.5}CoO_{3+\sigma}$ was prepared from the analytically pure oxides used appropriate stoichiometric proportion of La_2o_3, Gd_2O_3, Co_3O_4 and $SrCO_3$ by solid state reaction, after repeated grinding and sintering at 1250 °C for 24h for $La_{0.4}Gd_{0.1}Sr_{0.5}CoO_{3+\sigma}$. The LGSCO and ZnO layers were successively deposited on the single-crystal LAO (100) substrate by pulse laser deposition. The pulse laser was 248nm, frequency 5Hz, and pulse energy 150mJ. The LGSCO thin film about 220nm (estimated by SpecEI-2000-VIS ellipsometer) was deposited on $LaAlO_3$ (100) with the substrate kept at 800°C and oxygen pressure 10 Pa. The ZnO film bout 75nm was masked on $La_{0.4}Gd_{0.1}Sr_{0.5}CoO_{3+\sigma}$ (100). The structure of the target and the orientation of the deposited film were studied by XRD (Bruker D8 Advance XRD, 40KV, 40mA, Smallest angular step 0.0001^0). The sample of heterojunction thin film was placed in a JanisCCS-300 closed-circuit refrigerator cryostat (JanisCCS-300) and the measured temperature in ranged from 50 to 300 K. The magnetic field of 0.1, 0.3 and 0.5 T was supplied by the electromagnet perpendicularly applied to the heterostructure. The optical sources for photoexcitation were 155mW/cm^2 pulse wave laser and 200mW/cm^2 green-light wave.

The topography of $ZnO/La_{0.4}Gd_{0.1}Sr_{0.5}CoO_{3+\sigma}$ heterojunction was measured though the AFM image. The AFM surface morphology and phase field image for $ZnO/La_{0.4}Gd_{0.1}Sr_{0.5}CoO_3$/LAO and $ZnO/La_{0.4}Gd_{0.1}Sr_{0.5}CoO_{3+\sigma}$/Si were characterized by atomic resonance force microscopy (AFM), respectively.

3. Results and discussion

The LGSCO/ZnO structure was characterized by x-ray diffraction pattern at 180K shown in Fig. 1. The grain refinements showed LGSCO sample crystal belong to the hexagonal perovskite structures (space group:R-3C) with no more than 1% Co_3O_4 as the second phase. The XRD image indicated that the $La_{0.4}Gd_{0.1}Sr_{0.5}CoO_{3+\sigma}$ (100) and (200) diffraction peaks occurred at 2θ =32.8^{0}and 2θ =47.2^0, while the ZnO (100) (002) (101) (102) (110) (103) (200) diffraction peak occured at 2θ =31.59^0,2θ =34.37^0, 2θ =36.09^0, 2θ =47.3^0,2θ =56.4^0, 2θ =62.78^{0}and 2θ =66.15^0. Besides the spectrum peak showed orientation of LGSCO crystal plane, the diffraction peak of LAO (100), (200) substrate appear at 2θ =23^{0}and 2θ =47^0. This identified LGSCO film which was identical in the crystal plane orientation (100) with the LAO substrate had the multi-crystal structure. $La_{0.4}Gd_{0.1}Sr_{0.5}CoO_3$ XRD chart in 2θ =28^0 has GdO characteristic diffraction peak which showed doped Gd goes in to the LGSCO lattice. The diffraction peak of $ZnO/La_{0.4}Gd_{0.1}Sr_{0.5}CoO_3$ was matched with the LAO substrate (lattice constant 0.38769 nm) when the lattice constant was 0.386 and 0.379nm respectively. The results indicated that the $La_{0.4}Gd_{0.1}Sr_{0.5}CoO_3$ and ZnO thin films had better epitaxial characters respectively. The LaGdSrCoO3 average grain size of the film was 2.7 nm in coincidence with AFM results.

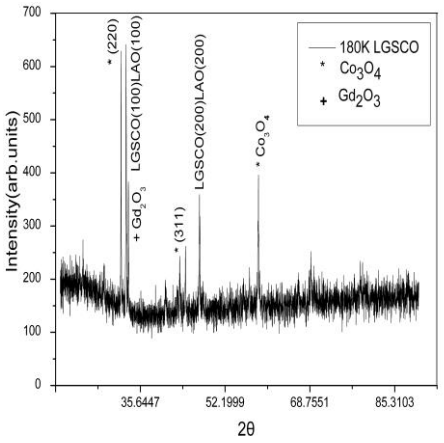

(a)

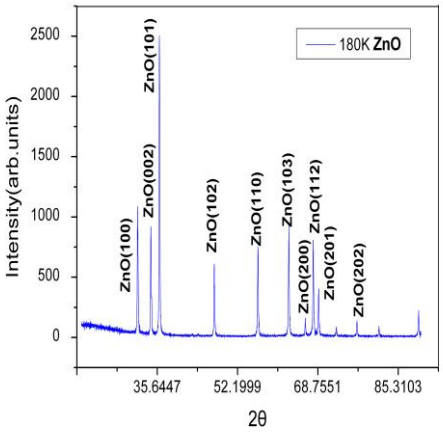

(b)

Fig.1 X-ray diffraction of $ZnO/La_{0.4}Gd_{0.1}Sr_{0.5}CoO_{3+\sigma}$/LAO heterostructure at 180K. The Figure (a) (b) shows the (100) and (200) peaks of the LGSCO film (a) and ZnO film (b).

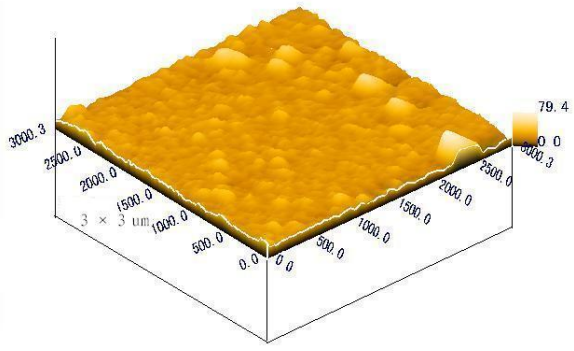

Fig.2. a. The AFM image (unit:nm) of surface morphology $ZnO/La_{0.4}Gd_{0.1}Sr_{0.5}CoO_{3+\sigma}$/LAO.

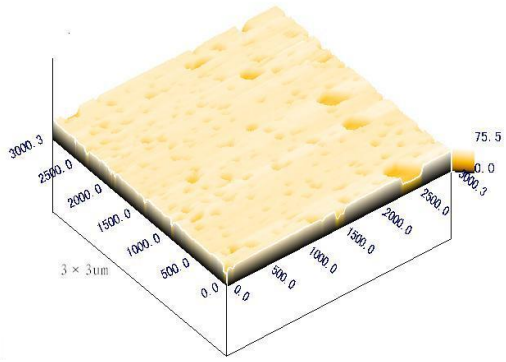

Fig. 2.b AFM phase field image(unit:nm) of the surface morphology ZnO/ $La_{0.4}Gd_{0.1}Sr_{0.5}CoO_{3+\sigma}$/LAO. The bright region is hard phase, and the dark region is soft phase.

Fig. 2a, AFM results were presented for ZnO/$La_{0.4}Gd_{0.1}Sr_{0.5}CoO_3$/LaAlO. ZnO/$La_{0.4}Gd_{0.1}Sr_{0.5}CoO_3$ film displayed a smooth surface with uniform grain size and the interface roughness of ZnO/$La_{0.4}Gd_{0.1}Sr_{0.5}CoO_3$ was about 2.7 nm due to LaAlO substrate. On the other hand, the carrier concentration measured from Hall effects of room temperature in the $La_{0.4}Gd_{0.1}Sr_{0.5}CoO_3$ and ZnO was determined by oxygen deficiency. We measured AFM phase field image of the surface morphology ZnO/ $La_{0.4}Gd_{0.1}Sr_{0.5}CoO_{3+\sigma}$/LAO shown in Fig. 2 b. The bright region was hard phase, and the dark region was soft phase.

Fig. 3 showed the setup illustration and I-V characteristics of a ZnO/$La_{0.4}Gd_{0.1}Sr_{0.5}CoO_{3+\sigma}$ junction at 240,260, and 300K. In this work, forward offset voltage was defined as a positive applied on the LGSCO film. The current-voltage (I-V) characteristics were measured and the biased current flowed from the LGSCO to the ZnO. The I-V properties of ZnO/$La_{0.4}Gd_{0.1}Sr_{0.5}CoO_{3+\sigma}$ for current applied perpendicular to the film surface were analysed at difference temperature. The rectifying characteristics of a p-n junction were displayed over a temperature range of 240-300k. The behavior was asymmetric structure with backword diode-like shape in the range of -8 to +8V. The I-V curves were very asymmetric characteristics at reverse and positive bias measured from T=240 K to 300 K. The I-V curve became steeper in the positive-bias and the negatives bias was less obvious than the positive bias from 300 to 240 K. Similar results had been reported in ZnO/$LaSrMnO_3$, ZnO/Si and ZnO/$SrTiO_3$ junction. [16,22] We observed rectifying electronic transport which suggested our heterojunction satisfy the Fletcher condition that depletion layer is less than width of space charge zone. It is found that the heterojunction at 300K had the highest slope of the I-V properties in the forward mode. The resistance result indicated that there exists two kinds of Schottky and ohmic contact between electrode interfaces at ZnO/LGSCO, and the slope denoted positive contact resistance. The generation of electron carriers was due to the photoexcitation ZnO. Furthermore, the junction voltage decreased and the potential barrier became thick. The electron tunneling made rectification characteristic reduced [14]. The similar phenomenon were identified in $SrTiO_3$/LCSCO/n-Si multi-junctions by H. B. Lu [16].

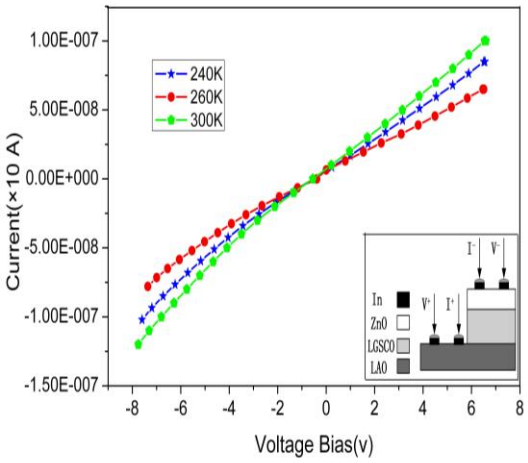

Fig. 3. I-V properties of the LAO/LGSCO/ZnO multi-p-n junction of various temperatures with the heterostructure current density curve demonstrate the rectifying behavior over a wide temperature of 240-300K. The inset is designed pattern ZnO/ $La_{0.4}Gd_{0.1}Sr_{0.5}CoO_{3+\sigma}$/LAO.

The temperature is dependence of the LGSCO/ZnO junction resistance under different applied magnetic field. Comparing with the resistance without an external magnetic field, the MR reduced with increasing temperature at 0.2T and 0.5T in experiment. The electrons transport and M-I transition in the films were spin-orbit coupling between localized electrons Co-3d t_{2g} and itinerant electrons O-2p e_g. The magnetoresistance is defined as MR=R/R=(R_H−R_O)/Ro where R_H is the resistance of heterojunction with the applied magnetic field, R_O is the resistance without the magnetic field. Over the range of temperature more than 150 K, the junction displayed a metallic-like in which there was temperature dependence of dR/dT<0. The junction at 0.2H and 0.5T became typically semiconducting below 100 and 125K, respectively. That Co-O-Co bond bending altered LGSCO to have an M-I transition boundary. Fig. 4 showed that the absolute value of the positive LGSCO/ZnO MR reduced monotonously with increasing temperature, and the MR of 100 K went up 5.32% at 0.5T, 4.62% at 0.2T, while MR deceased about 3.16% at 0.5T, 300 K and 2.42% at 0.2T, 300K. Comparing with the MR-T curve from 0.2 to 0.5T, the magnetic resistance became larger with increasing magnetic field. Moreover, the phase transition of junction from ferromagnetic metal to paramagnetic insulator occurred at Curie temperature Tc .

Fig. 4 displayed the photoresistance dependence of temperature at difference intensity lasers. The photo resistances were decreased with increasing temperature over the range of T<200K. The negative photoresistance was observed in bath irradiated LGSCO single layer and

double irradiated ZnO/LGSMO layer. The photocarrier transfer in irradiated ZnO/LGSMO was increased more than in irradiated LGSMO single layer. The PR of double irradiated ZnO/LGSMO at laser light 200 mW/cm^2 was reduced by 33.33% of the original resistance. Meanwhile, the PR of irradiated LGSMO single layer at pulse laser 155 mW/cm^2 was reduced by 5% of the resistance. The peak values were slightly depressed from ~33.33% for double irradiated ZnO/LGSMO layers to ~5% for single irradiated LGSMO layer. Similar characteristics were identified in the $La_{0.75}Sr_{0.25}Co_{0.25}O_{3+\sigma}$ and $La_{0.7}Y_{0.05}Sr_{0.25}Co_{0.25}O_3$. The magnetic field led to MI transition at the low temperature, and the light generated photoinduced demagnetization control carriers transport in $La_{0.8}Sr_{0.2}Co_{0.5}N_{i0.5}O_3$/ZnO films using an epitaxial ZnO:Al/LGSCO film.[19] This characteristics were also displayed by HB Lu and Park J.H. who found LSMO Femi energy band broken at temperature 40K.[20] ZnO/$La_{0.4}Gd_{0.1}Sr_{0.5}CoO_{3+\sigma}$ junction has potential properties of piezoelectric, ferroelectric, thermoelectric, and optoelectronic in heterostructure [21,22].

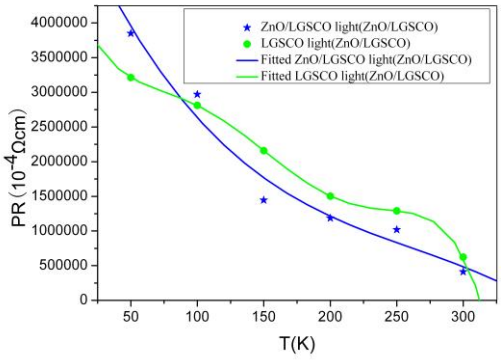

Fig. 4. The temperature dependence of the junction resistance with applied light field and photoinduced resistance characteristics.

4. Conclusions

In summary, we have shown the leakage mechanism of ZnO/$La_{0.4}Gd_{0.1}Sr_{0.5}CoO_{3+\sigma}$ with asymmetric electrodes on LAO substrates to be dominated by Poole-Frenkel emission. The obvious photoinduced resistance characteristics from ~33.3% for double irradiated ZnO/LGSMO layers to ~5% for single irradiated LGSMO layer and positive MR effect are observed to increase 5.32% at 0.5T and 4.62% at 0.2T,100 K in the ZnO/$La_{0.4}Gd_{0.1}Sr_{0.5}CoO_{3+\sigma}$/LaAlO heterostructure. The ZnO/ LGSCO junction exhibited the carrier transfer of MIT transition and photoinduced demagnetization at different temperatures. Our measure is attributed to the further understanding of charge order, spin-orbital coupling, magnetic order, and optical field from the view of development and application of photoinduced manganites and positive CMR device.

Acknowledgements

This work is supported by NSFC (10775111),MOE Key Laboratory for Nonequilibrium Condensed Matter and Education Foundation of China 2009 (Grant No. 2009, 1001).

References

[1] R. Vonhelmolt, J. Wecker, K. Samwer, L. Haupt, K. Barner, J. Appl. Phys. **76**, 6925 (1994).
[2] R. Vonhelmolt, J. Wecker, B. Holzapfel, L. Schultz, K. Samwer, Phys. Rev. Lett. **71**, 2331 (1993).
[3] C. Zener, Phys. Rev. **82**,403 (1951).
[4] G.. C. Xiong, B. Zhang, S. C. Wu, Z. X. Lu, J. F. Kang, G. J. Lian, D. S. Dai, Solid State Comm. **97**, 17 (1996).
[5] G. H. Jonker, J. Appl. Phys. **37,** 1424 (1966).
[6] R. Lengsdort, M. Ait-Tahar, S. S. Saxena et al, Phys. Rev. B. **69**, 140403 (2004).
[7] M. Kriener, C. Zobel a Reichl et al physical Rev. B, **69**, 94417 (2004).
[8] S. Jin, T. H. Tiefel, M. McCormack, R. A. Fastnacht, R. Ramesh, L.H. Chen, Science **264**, 413 (1994)
[9] R. Ren, X. K. Qin, W. R. Wang, Rare Metal Materials and Engineering, **42**(1), 140 (2013).
[10] A. Chainani, M. Mathew, D. D. Sarma, Phys. Rev. B. **46**, 9976 (1992).
[11] H. Tanaka, J. Zhang, T. Kawai, Phys. Rev. Lett. **88**, 027204 (2002).
[12] W. Luo, F. Shi, F. Wang, J. Magnetism and Magnetic Material, **305**, 509 (2006).
[13] R. Ren, C. L. Chen, Zhu S. H., Physica Scripta, **72(1)**, 87-90 (2005).
[14] J. Wu, X. Lou, Y. Wang, J. Wang, Electrochem. Solid-State Lett. **13**, 2 (2010).
[15] G. W. Pabst, L. W. Martin, Y.-H. Chu, R. Ramesh, Appl. Phys. Lett. **90**, 072902 (2007).
[16] R. Ren, C. L. Chen, Plasma Science & Technology, **8**(5), 561 (2006).
[17] X. P. Zhang, B. T. Xie, Y. S. Xiao, B. Yang, P. L. Lang, Y. G. Zhao, Appl. Phys. Lett., **87**, 072506 (2005).
[18] C. Mitra, P. Raychaudhuri, K. Dörr, K. H. Muller, L. Schultz, P. M. Oppeneer, S. Wirth, Phys. Rev. Lett. **90**, 017202 (2003).
[19] Ren R, W. R. Wang, Journal of Computational and Theoretical Nanosicence, **9**, 1622 (2012).
[20] Y. C. Wang, R. Ren, C. L. Chen, Canadian Journal of Physics, **83**(7), 699 (2005).
[21] Ala'Eddin A. Saif, P. Poopalan, Optoelectron. Adv. Mater. Rapid Commun. **4**(12), 2008 (2010).
[22] Z. Z Lazarevic, S Kostic, V. Radojevic, Optoelectron. Adv. Mater. Rapid Commun. **7**(1-2), 58 (2013).

*Corresponding author: ren@mail.xjtu.edu.cn